

# Original Article

*Journal of Cerebral Blood Flow & Metabolism* (1999) **19**, 272–277; doi:  
10.1097/00004647-199903000-00005

## Frequency-Dependent Changes in Cerebral Metabolic Rate of Oxygen During Activation of Human Visual Cortex

Supported by Medical Research Council of Canada grant SP-30, the Isaac Walton Killam Fellowship Fund of the Montreal Neurological Institute, the McDonnell-Pew Program in Cognitive Neuroscience, and Medical Research Council (Denmark) grants 12-1633 and 12-1634.

Manouchehr S Vafae, Ernst Meyer, Sean Marrett, T Paus, Alan C Evans and Albert Gjedde

McConnell Brain Imaging Centre, Positron Emission Tomography Laboratories, Montreal Neurological Institute, McGill University, Montreal, Quebec, Canada

Correspondence: Manouchehr S Vafae, McConnell Brain Imaging Centre, Montreal Neurological Institute, 3801 University Street, Montreal, Quebec, Canada H3A 2B4.

Received 12 December 1997; Revised 22 April 1998; Accepted 24 April 1998.

### Abstract

To test the hypothesis that brain oxidative metabolism is significantly increased upon adequate stimulation, we varied the presentation of a visual stimulus to determine the frequency at which the metabolic response would be at maximum. The authors measured regional  $CMR_{O_2}$  in 12 healthy normal volunteers with the ECAT EXACT HR+ (CTI/Siemens, Knoxville, TN, U.S.A.) three-dimensional whole-body positron emission tomograph (PET). In seven successive activating conditions, subjects viewed a yellow-blue annular checkerboard reversing its contrast at frequencies of 0, 1, 4, 8, 16, 32, and 50 Hz. Stimulation began 4 minutes before and continued throughout the 3-minute dynamic scan. In the baseline condition, the subjects began fixating a cross hair 30 seconds before the scan and continued to do so for the duration of the 3-minute scan. At the start of each scan, the subjects inhaled 20 mCi of  $^{15}O-O_2$  in a single breath. The  $CMR_{O_2}$  value was calculated using a two-compartment, weighted integration method. Normalized PET images were averaged across subjects and coregistered with the subjects' magnetic resonance imaging in stereotaxic space. Mean subtracted image volumes (activation minus baseline) of  $CMR_{O_2}$  then were obtained and converted to  $z$  statistic volumes. The authors found a statistically significant focal change of  $CMR_{O_2}$  in the striate cortex ( $x = 9$ ;  $y = -89$ ;  $z = -1$ ) that reached a maximum at 4 Hz and dropped off sharply at higher stimulus frequencies.

### Keywords:

$CMR_{O_2}$ , Visual cortex, Positron emission tomography

## Abbreviations:

ANOVA, analysis of variance; MRI, magnetic resonance imaging; PET, positron emission tomography

The human brain consumes glucose and oxygen to sustain its function. The substrates are continuously supplied through the cerebral circulation, which supplies 20% of the cardiac output. The mechanism linking neuronal activity to the circulation generally is believed to constitute a flow-metabolism couple. This couple is thought to satisfy the principle of [Roy and Sherrington \(1890\)](#), which has been interpreted to mean that CBF changes must subservise a tight coupling between cellular energy requirements and the supplies of glucose and oxygen to the brain ([Gjedde, 1997](#)). The homeostatic mechanism maintains a constant concentration of ATP, the compound that ties the processes that deplete the energy potential of brain tissue to those that restore it. Several investigators have demonstrated that CBF in the brain is tightly coupled to the metabolic requirements of tissue for glucose and oxygen, that is,  $CMR_{glc}$  and  $CMR_{O_2}$  ([Siesjö, 1978](#); [Yarowsky and Ingvar, 1981](#)).

Recent studies report a mismatch between changes of CBF and oxygen use during functional activation of the human brain despite a match between changes of regional glucose consumption and CBF ([Fox and Raichle, 1986](#); [Fox et al., 1988](#); [Fujita et al., 1992, 1999](#); [Ribeiro et al., 1993](#)). These findings constitute a significant departure from the original principle formulated by Roy and Sherrington. However, in this laboratory, we have observed significant increases of  $CMR_{O_2}$  in the striate cortex in response to a visual stimulation ([Marrett et al., 1995](#); [Vafaei et al., 1996, 1998](#); [Marrett and Gjedde, 1997](#)) along with a commensurate elevation of CBF. In these studies, the  $CMR_{O_2}$  response to a single stimulation frequency, namely 8 Hz, which had provided a maximum response in previous CBF studies ([Fox and Raichle, 1984, 1985](#)), was compared with a resting baseline. In the current experiment, we examined changes in  $CMR_{O_2}$  as a function of stimulus frequency (tuning curve).

Knowledge of the  $CMR_{O_2}$  response to the rate of stimulation is required to evaluate the so-called oxidative index, defined as the  $CMR_{O_2}/CBF$  ratio. This index yields new information about the degree of oxidative breakdown of glycolysis prevailing in specific areas of the brain during physiologic stimulation. The current experiment determines the frequency dependence of  $CMR_{O_2}$  changes by means of a previously tested visual stimulus, a yellow-blue contrast reversing checkerboard. We have already shown that this stimulus was capable of giving rise to changes of  $CMR_{O_2}$  in the visual cortex ([Marrett et al., 1995](#); [Vafaei et al., 1996, 1998](#); [Marrett and Gjedde, 1997](#)).

## MATERIALS AND METHODS

Twelve healthy normal volunteers (6 men and 6 women), aged between 22 and 32 years (mean  $\pm$ SD, 25  $\pm$ 3.5 years), were studied for this protocol approved by the Research Ethics Committee of the Montreal Neurological Institute and Hospital. Informed written consent was obtained from each volunteer.

### Positron emission tomography measurement

Positron emission tomography (PET) studies were performed on the ECAT EXACT HR+ (CTI/Siemens) whole-body tomograph, operating in a three-dimensional acquisition mode, with a transverse resolution of 4.5 to 5.8 mm and an axial resolution of 4.9 to 8.8 mm ([Adam et al., 1997](#)). The images were reconstructed as 128  $\times$  128 matrices of 2 mm  $\times$  2 mm pixels

using filtered back-projection with an 8-mm Hanning filter (full width at half maximum). Reconstructed images were corrected for random and scattered events, detector efficiency variations, and dead time. Three orbiting rod transmission sources, each containing about 5 mCi of  $^{68}\text{Ge}$ , were used for attenuation correction.

The subjects were positioned in the tomograph with their heads immobilized by means of a customized head holder (Vac-Lock, MED-TECH). A short indwelling catheter was placed into the left radial artery for blood sampling and blood gas examination. Arterial blood radioactivity was automatically sampled, corrected for delay and dispersion ([Vafaei et al., 1996](#)), and calibrated with respect to the tomograph using samples obtained manually during the last 60 seconds of each 3-minute scan. At the start of each scan, the subjects inhaled 20 mCi of  $^{15}\text{O}-\text{O}_2$  in a single breath. The  $\text{CMR}_{\text{O}_2}$  was calculated using the two-compartment, weighted integration method ([Ohta et al., 1992](#)). Each subject also underwent a magnetic resonance imaging (MRI) examination on a Philips Gyroscan ACS (1.5 T) superconducting magnet system for structural-functional (MRI-PET) correlation. The MRI image was a T1-weighted, three-dimensional fast field echo sequence consisting of 160 256  $\times$  256 sagittal slices of 1-mm thickness.

### **Stimulus conditions**

The stimulus was generated with a Silicon Graphics (SGI) work station and presented using a 53-cm (21-inch) NEC monitor (MultiSync XP21) with a synchronization range of 31 to 89 kHz (horizontal) and 55 to 160 Hz (vertical), and a temporal resolution of 55 to 83 Hz. It consisted of a yellow-blue annular checkerboard with an outer diameter of 13.5 cm and an inner diameter of 0.5 cm. It contained six concentric rings, each ring consisting of a total of 36 segments of equal size, alternating in intensity (yellow and blue). The dimensions of the outermost segments were 8 mm peripherally and 12 mm axially. A cross hair (0.5 cm) was located at the center of the circle. The stimulus was presented at about 17 degrees of visual angle (40 to 45 cm from the eyes), and its contrast was reversing at specified frequencies. In the baseline condition, the subjects were asked to fixate on a cross hair in the center of the screen 30 seconds before the scan and throughout the subsequent 3-minute scan. In seven successive activation conditions, the subjects were shown a yellow-blue annular checkerboard reversing its contrast at frequencies of 0, 1, 4, 8, 16, 32, and 50 Hz. Six of the subjects were shown the stimulus in ascending order (baseline, 0, 1, 4, 8, 16, 32, and 50 Hz) whereas the other six were shown the stimulus in descending order (baseline, 50, 32, 16, 8, 4, 1, and 0 Hz). Stimulation began 4 minutes before the start of the dynamic PET scan and continued throughout the following 3-minute scan for a total of 7 minutes. There was a minimum of 15 minutes' time gap between each scan. Black drapes were used to create a dark environment around the screen.

### **Data analysis**

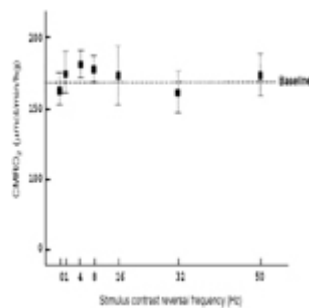
The magnetic resonance images were transformed into stereotaxic coordinates ([Talairach and Tournoux, 1988](#)) using an automatic registration algorithm ([Collins et al., 1994](#)). The reconstructed PET images were coregistered with the subjects' MRI scans using an automatic registration program based on the automatic image registration algorithm ([Woods et al., 1992](#)). For this purpose, the sum of the PET images across all frames was calculated for each scan. The MRI image then was aligned with the summed PET image. To correct for between-scan subject movements, automatic PET-to-PET registration also was performed ([Woods et al., 1993](#)). This method uses the first PET scan (summed across frames) as the registration target for each subsequent summed PET scan. The global cerebral metabolic rates of oxygen ( $\text{CMR}_{\text{O}_2}$ ) were determined for each subject by means of a binarized brain mask, which filters out all extracerebral voxels. This mask was created by thresholding and manually editing the

average MRI of 305 normal brains scanned at the Montreal Neurological Institute. The global  $CMR_{O_2}$  for each subject then was determined by averaging the values of all intracerebral voxels. The reconstructed PET images then were normalized for global  $CMR_{O_2}$  and averaged across subjects, transformed into stereotaxic coordinates, and blurred with a Gaussian filter of 22 mm  $\times$  22 mm  $\times$  22 mm. Mean subtracted image volumes (stimulation minus baseline) were obtained and converted to  $z$  statistic volumes by dividing each voxel by the mean SD of the normalized subtraction image obtained by pooling the SD across all intracerebral voxels. Significant focal changes of  $CMR_{O_2}$  were identified by a method based on three-dimensional Gaussian random field theory (Worsley et al., 1996). Values equal to or exceeding a criterion of  $z = 3.5$  were deemed statistically significant ( $P < 0.00046$ , two-tailed, uncorrected). Correcting for multiple comparison, a  $z$  value of 3.5 yields a false-positive rate of 0.26 in 70 resolution elements, each of which has dimensions of 22  $\times$  22  $\times$  22 mm<sup>3</sup>. This approximates the total volume of brain scanned (2.2  $\times$  2.2  $\times$  2.2  $\times$  70 = 750 cm<sup>3</sup>).

## RESULTS

The mean global  $CMR_{O_2}$  values of the 12 subjects at the seven stimulus frequencies are shown in Fig. 1. A one-factor analysis of variance (ANOVA) showed that there was no significant effect of scanning condition on  $CMR_{O_2}$  ( $F = 0.15$ ;  $P > 0.5$ ).

**Figure 1.**

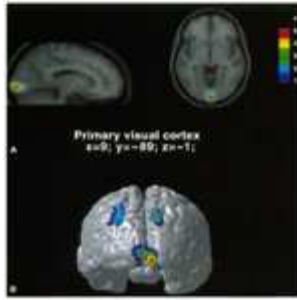


Change in global  $CMR_{O_2}$  ( $\pm$  SD) as a function of checkerboard contrast reversal frequency.

[Full figure and legend \(43K\)](#)

In contrast, regional  $CMR_{O_2}$  in primary visual cortex (Fig. 2) varied as a function of stimulus frequency. As shown in Fig. 3,  $CMR_{O_2}$  in primary visual cortex increased as the stimulus frequency increased, peaking at 4 Hz, and then dropped off sharply at higher frequencies. Table 1 shows the  $z$  values and  $P$  values for significant peaks obtained for different frequencies. A one-factor ANOVA performed on the absolute regional  $CMR_{O_2}$  values derived from a region of interest (primary visual cortex) for all frequencies resulted in  $F = 3.55$  and  $P < 0.05$ , thus confirming that there is a significant difference between those values. In addition, post hoc pairwise comparisons were performed on the absolute  $CMR_{O_2}$  values using a paired  $t$  test. As a result, a statistically significant difference was found between the values of 4 and 1 Hz ( $P < 0.05$ ). The test also showed that there is no significant difference between the values of 0 and 8 Hz ( $P = 0.7$ ), whereas there were significant differences between the  $CMR_{O_2}$  values for these frequencies and those at 1 Hz ( $P < 0.005$ ). Moreover, the test showed that there were no significant differences between the  $CMR_{O_2}$  values of 16, 32, and 50 Hz ( $P = 0.98$ ).

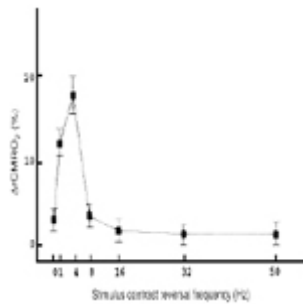
**Figure 2.**



Averaged positron emission tomography (PET) subtraction images of  $CMR_{O_2}$  superimposed on averaged magnetic resonance images. Subtraction of control from activation state yielded the focal changes in  $CMR_{O_2}$ , shown as  $z$  statistic images. **(A)** The focal  $CMR_{O_2}$  changes in primary visual cortex (occipital pole) is shown for a frequency of 4 Hz. **(B)** A PET  $CMR_{O_2}$  image superimposed on averaged, rendered magnetic resonance image is shown (4 Hz).

[Full figure and legend \(415K\)](#)

**Figure 3.**



Change in regional  $CMR_{O_2}$  ( $\pm$  SD) in primary visual cortex as a function of checkerboard contrast reversal frequency.

[Full figure and legend \(27K\)](#)

**Table 1 - Z values and corresponding P values of significant activation peaks in primary visual cortex (stimulation – baseline) in response to stimulation by yellow-blue checkerboard (x = 9; y = -89; z = -1).**

[Full table](#)

We ascertained that the order of presentation of the stimulus did not alter the final values of  $CMR_{O_2}$  (global and regional) by performing a two-factor ANOVA. The test showed that there was no statistically significant difference between the  $CMR_{O_2}$  values when stimulus frequency was presented in different orders ( $F = 0.38$ ;  $P > 0.5$ ).

## DISCUSSION

A direct relation between stimulation rate and cerebral metabolic rate of glucose ( $CMR_{glc}$ ) has been reported in both the peripheral nervous system ([Toga and Collins, 1981](#)) and the CNS of rats ([Yarowsky et al., 1983](#)). The effect of stimulus rate on CBF in humans also was studied by several investigators. Studies of human auditory cortex have shown a linear dependence of CBF on the rate of auditory stimulation ([Price et al., 1992](#)). In addition, in the motor system, different repetition rates of finger and eye movements have led to rate-dependent changes in CBF ([Sadato et al., 1996](#); [Paus et al., 1995](#)). In this laboratory, we also have observed a linear relation between the direct stimulation of the human cerebral cortex by means of transcranial magnetic stimulation and regional CBF ([Paus et al., 1997](#)). Moreover, the relation between stimulation rate and CBF change in human visual cortex has been investigated using PET ([Fox and Raichle, 1984, 1985](#)).

This study determined which relation, if any, existed between frequency as an indicator of neuronal work and regional  $CMR_{O_2}$  as an index of oxidative metabolism. In essence, we tested the hypothesis that oxidative metabolism must be elevated when activated by an adequate stimulus, "adequate" classically referring to the stimulus to which the system responds maximally.

Biochemical evidence suggests that visual neurons differ in their capacity to sustain oxidative phosphorylation. The staining pattern in primary visual cortex (V1) for the mitochondrial enzyme cytochrome oxidase ([Horton, 1984](#); [Wong-Riley and Carroll, 1984](#)) reflects such a specialization. This pattern reveals an organization of neurons in the superficial layers III and II into the so-called "blobs" and "interblobs." We showed previously that after the activation of visual cortex with a chromatically rich stimulus (i.e., a yellow-blue reversing checkerboard),  $CMR_{O_2}$  rose markedly in primary visual cortex ([Marrett et al., 1995](#); [Vafaei et al., 1996, 1998](#); [Marrett and Gjedde, 1997](#)). The high abundance in the visual cortex of color-sensitive neurons rich in cytochrome oxidase was a possible explanation for this finding. These measurements of  $CMR_{O_2}$  were made after sustained (7 minutes) stimulation of the visual cortex. The observed increases in  $CMR_{O_2}$  appeared to be stimulus specific, since simple photic stimulation with Grass eye goggles (i.e., an array of red light emitting diodes flashing at 8 Hz) failed to induce significant increases of  $CMR_{O_2}$  ([Fujita et al., 1992, 1993](#); [Ribeiro et al., 1993](#)). Since the same method of  $CMR_{O_2}$  determination was used in the latter studies, the observed increases in  $CMR_{O_2}$  in the visual cortex might be associated with the ability of the chromatically rich stimulus to activate the cytochrome oxidase-rich neurons (blobs), which seem to be involved in color processing.

It has been reported that the response of retinal ganglion cells directly depends on the temporal frequency of the flicker ([Henkes and Van Der Tweel, 1964](#); [Schickman, 1981](#)). The term *flicker* was referred to as a pattern of illumination on the retina, some portion of it being turned on and off or having its intensity modulated with time. [Bartley in 1937](#) studied the retinal response through optic nerve discharges and found that, as the interval between successive photic pulses was shortened, the latency of discharges was lengthened ([Bartley, 1937, 1968](#)). This continued up to a certain rate, then as the intervals between pulses were further shortened, the latency began to decrease. Bartley assumed that this phenomenon was evidence for the receptor-bipolar-ganglion cell chains being able to follow the input rate only up to certain limit. Other investigators also have demonstrated that after electric and photic stimulation of postretinal visual structures, evoked potentials of the visual system became a function of temporal frequency of stimulation ([Bartley, 1968](#); [Movshon et al., 1978](#)) which, in humans, peaked around the alpha-rhythm activity of 8 to 10 Hz. The frequency-dependent changes of blood flow in visual cortex reported by Fox and Raichle are in agreement with the



fact that CBF is an index of neuronal activity, and their finding that CBF peaks around 8 Hz is a confirmation for the findings discussed earlier.

Our results show that for the current stimulus,  $CMR_{O_2}$  in the visual cortex varies as a function of stimulus frequency. Unlike regional CBF, which has been observed to peak at 8 Hz ([Fox and Raichle, 1984, 1985](#)), regional  $CMR_{O_2}$  in this study reached its peak at 4 Hz and dropped off at higher frequencies. Based on our findings, we speculate that two limitations may operate in the tissue. A primary limitation (physiologic) is imposed by the finite oxygen diffusibility in the brain tissue ([Kassissia et al., 1995](#)). This limitation is a result of the barrier-limited oxygen transfer to brain across cerebral capillaries. From human studies showing increased blood flow during stimulation of visual cortex (Fox et al., 1985; Marrett et al., 1997), we hypothesize that this limitation is overcome when blood flow increases sufficiently to raise the average oxygen tension in capillary blood. However, previous studies also have shown that even when the limit to increased oxygen delivery has been lifted by an increase of blood flow, oxygen consumption does not always rise under conditions accompanied by increased blood flow. We speculate that this secondary limitation (enzymatic) represents a cellular mechanism that causes the brain not to fully sustain the increase of  $CMR_{O_2}$  made possible by the blood flow increase. The current results suggest that such a secondary limitation could be overcome by increasing the stimulus load. In this context, the term stimulus *load* refers to the integration of the stimulus effects on the system as a function of time and intensity. We, therefore, hypothesize that a blood flow increase accompanying the stimulus frequency of 4 Hz permits the  $CMR_{O_2}$  to increase to the observed value. When the frequency of the stimulus increases above 4 Hz, neuronal work no longer requires the  $CMR_{O_2}$  to rise. Thus, we claim that the two limitations appear to operate in the tissue are a limitation that is lifted in proportion to stimulus load, the variable which integrates length, strength, and kind of stimulation applied after a basic oxygen diffusibility limitation, which is lifted when blood flow is raised.

Notice that we had previously reported a significant  $CMR_{O_2}$  change at 8 Hz with the same visual stimulus ([Vafaei et al., 1996, 1998](#)). That study, however, had been carried out using a single stimulation frequency (8 Hz), unlike the current experiment, which was especially designed to explore the frequency response (tuning curve) to the same visual stimulus used before. Furthermore, the previous study was performed on an older, two-dimensional acquisition tomograph (Scanditronix PC-2048 15B) whereas for the current study, a state-of-the-art three-dimensional machine (ECAT EXACT HR+CTI/Siemens) with a five to seven times larger sensitivity was used. Therefore, the Gaussian filter, which was used to enhance the signal-to-noise ratio of an image (because of low count rates), was not the same for the two studies, given the entirely different noise characteristics of the two machines (two- versus three-dimensional). As a consequence, the  $CMR_{O_2}$  change at 8 Hz in the current study failed to be significant, although the activation peaks were apparent on visual inspection.

In conclusion, the ability of brain neurons to increase oxygen use may depend on the specific task that the neurons perform, and the stimulus load imposed on the brain tissue must exceed a certain threshold before glycolysis is augmented by increased oxidative metabolism.

## References

1. Adam LE, Zaers J, Ostertag H, Trojan H, Bellemann ME, Brix G & Lorenz WJ. (1997) Performance evaluation of the whole-body PET scanner ECAT EXACT HR+. *Proc IEEE* **2**: 1270–1274.
2. Bartley SH. (1937) Some observations on the organization of the retinal response. *Am J Physiol* **120**: 184.

3. Bartley SH. 1968 Temporal features of input as crucial factors in vision. (In) *Contributions to Sensory Physiology*, Vol. 3 (Neff WD, ed) New York, Academic Press (pp) 81–124. | [ChemPort](#) |
4. Collins DL, Neelin P, Peters TM & Evans AC. (1994) Automatic 3D intersubject registration of MR volumetric data in standardized Talairach space. *J Comput Assist Tomogr* **18**: 192–205. | [ChemPort](#) |
5. Fox PT & Raichle ME. (1984) Stimulus rate dependence of regional blood flow in human striate cortex, demonstrated by positron emission tomography. *J Neurophysiol* **51**: 1109–1120. | [PubMed](#) | [ISI](#) | [ChemPort](#) |
6. Fox PT & Raichle ME. (1985) Stimulus rate determines regional blood flow in striate cortex. *Ann Neurol* **17**: 303–305. | [Article](#) | [PubMed](#) | [ChemPort](#) |
7. Fox PT & Raichle ME. (1986) Focal physiological uncoupling of cerebral blood flow and oxidative metabolism during somatosensory stimulation in human subjects. *Proc Natl Acad Sci USA* **83**: 1140–1144. | [PubMed](#) | [ChemPort](#) |
8. Fox PT, Raichle M, Mintun M & Dence C. (1988) Nonoxidative glucose consumption during focal physiologic neuronal activity. *Science* **241**: 462–464. | [PubMed](#) | [ISI](#) | [ChemPort](#) |
9. Fujita H, Kuwabara H, Ohta S, Ribeiro L, Rajagopal S, Marrett S, Evans AC, Meyer E & Gjedde A. 1992 Evidence for stimulus-specific changes in oxidative metabolism. (In: *Proceedings, 6th Annual Turku Conference on the Medical Application of Cyclotrons*, May 1992, Turku, Finland).
10. Fujita H, Kuwabara H, Reutens DC & Gjedde A. (1999) Oxygen consumption of cerebral cortex fails to increase during continued vibrotactile stimulation. *J Cereb Blood Flow Metab* **19**: 266–271. | [Article](#) | [PubMed](#) | [ChemPort](#) |
11. Gjedde A. 1997 The relation between brain function and cerebral blood flow and metabolism. (In) *Cerebrovascular Disease* (Hunt Batjer H, ed) Philadelphia, Lippincott-Raven Publishers (pp) 23–40.
12. Henkes HE & Van Der Tweel LH. (1964) Flicker. *Doc Ophthalmol* **18**: 1–35.
13. Horton JC. (1984) Cytochrome oxidase patches: a new cytoarchitectonic feature of monkey visual cortex. *Philosophical Trans R Soc London B* **304**: 199–253. | [ChemPort](#) |
14. Kassissia IG, Goresky CA, Rose CP, Schwab AJ, Simard A, Huet PM & Bach GG. (1995) Tracer oxygen distribution is barrier-limited in the cerebral microcirculation. *Cir Res* **77**: 1201–1211. | [ChemPort](#) |
15. Marrett S, Meyer E, Kuwabara H, Evans AC & Gjedde A. (1995) Differential increases of oxygen metabolism in visual cortex. *J Cereb Blood Flow Metab* **15**: S80.
16. Marrett S & Gjedde A. (1997) Changes of blood flow and oxygen consumption in visual cortex of living humans. *Adv Exp Med Biol* **413**: 205–208. | [PubMed](#) | [ChemPort](#) |
17. Movshon JA, Thompson ID & Tolhurst DJ. (1978) Spatial and temporal contrast sensitivity of neurones in areas 17 and 18 of cat's visual cortex. *J Physiol London* **283**: 101–120. | [PubMed](#) | [ChemPort](#) |
18. Ohta S, Meyer E, Thompson CJ & Gjedde A. (1992) Oxygen consumption of the living human brain measured after a single inhalation of positron emitting oxygen. *J Cereb Blood Flow Metab* **12**: 179–192. | [PubMed](#) | [ChemPort](#) |
19. Paus T, Marrett S, Worsley KJ & Evans AC. (1995) Extraretinal modulation of cerebral blood flow in the human visual cortex: implications for saccadic suppression. *J Neurophysiol* **12**: 179–192.
20. Paus T, Jech R, Thompson CJ, Comeau R, Peters T & Evans AC. (1997) Transcranial magnetic stimulation during positron emission tomography: a new method for studying connectivity of the human cerebral cortex. *J Neurosci* **17**: 3178–3184. | [PubMed](#) | [ISI](#) | [ChemPort](#) |



21. Price C, Wise R, Friston K, Howard D, Patterson K & Frackowiak R. (1992) Regional response differences within the human auditory cortex when listening to words. *Neurosci Lett* **146**: 179–182. | [Article](#) | [PubMed](#) | [ChemPort](#) |
22. Ribeiro L, Kuwabara H, Meyer E, Fujita H, Marrett S, Evans AC & Gjedde A. 1993 Cerebral blood flow and metabolism during nonspecific bilateral visual stimulation in normal subjects. (In) *Quantification of Brain Function: Tracer Kinetics and Image Analysis in Brain PET* (Uemura K, Lassen NA, Jones T, Kanno I, eds) Amsterdam, Elsevier 229–234.
23. Roy CS & Sherrington CS. (1890) On the regulation of the blood supply of the brain. *J Physiol* **11**: 85–108.
24. Schickman GM. 1981 Time-dependent function in vision. (In) *Adler's Physiology of the Eye* (7th ed (Moses RA, ed)) St. Louis, Mosby (pp) 666–693.
25. Sadato N, Ibanez V, Deiber MP, Campbell G, Leonardo M & Hallett M. (1996) Frequency-dependent changes of regional cerebral blood flow during finger movements. *J Cereb Blood Flow Metab* **16**: 23–33. | [PubMed](#) | [ChemPort](#) |
26. Siesjö BK. 1978 *Brain Energy Metabolism* New York, Wiley.
27. Talairach J & Tournoux P. 1988 *Co-planar Stereotactic Atlas of the Human Brain: 3-Dimensional Proportional System, an Approach to Cerebral Imaging* Stuttgart, George Thieme Verlag.
28. Toga AW & Collins RW. (1981) Metabolic response of optical centers to visual stimuli in the albino rat: anatomical and physiological considerations. *J Comp Neurol* **199**: 443–464. | [Article](#) | [PubMed](#) | [ChemPort](#) |
29. Vafae MS, Murase K, Gjedde A & Meyer E. 1996 Dispersion correction for automatic sampling of O-15 labeled H<sub>2</sub>O and red blood cells. (In) *Quantification of Brain Function Using PET* (Myers R, Cunningham VJ, Bailey DL, Jones T, eds) San Diego, Academic Press (pp) 72–75. | [ChemPort](#) |
30. Vafae MS, Paus T, Gjedde A, Evans AC, Ptito A & Meyer E. (1996) Oxidative metabolism in human visual cortex during physiological activation studied by PET. *Soc Neurosci Abstr* **22**: 1060.
31. Vafae MS, Meyer E, Marrett S, Evans AC & Gjedde A. (1998) Increased oxygen consumption in human visual cortex: response to visual stimulation. *Acta Neurol Scand* **98**: 85–89. | [PubMed](#) | [ChemPort](#) |
32. Wong-Riley M & Carroll E. (1984) The effect of impulse blockage on cytochrome oxidase activity in the monkey visual system. *Nature* **307**: 262–264. | [Article](#) | [PubMed](#) | [ChemPort](#) |
33. Woods RP, Cherry SR & Mazziotta JC. (1992) Rapid automated algorithm for aligning and reslicing PET images. *J Comput Assist Tomogr* **16**: 620–633. | [PubMed](#) | [ISI](#) | [ChemPort](#) |
34. Woods RP, Mazziotta JC & Cherry SR. (1993) MRI-PET registration with automated algorithm. *J Comput Assist Tomogr* **17**: 536–546. | [PubMed](#) | [ISI](#) | [ChemPort](#) |
35. Worsley KJ, Marrett S, Neelin P, Vandal AC, Friston K & Evans AC. (1996) A unified statistical approach for determining significant signals in images of cerebral activation. *Human Brain Mapping* **4**: 58–73.
36. Yarowsky PJ & Ingvar DH. (1981) Neuronal activity and energy metabolism. *Fed Proc* **40**: 2358–2363.
37. Yarowsky PJ, Kadakara M & Sokoloff L. (1983) Frequency-dependent activation of glucose utilization in the superior cervical ganglion by electrical stimulation of cervical sympathetic trunk. *Proc Natl Acad Sci USA* **80**: 4179–4183. | [PubMed](#) | [ChemPort](#) |